

## Article

# Siphon-Induced Droplet Break-Off for Enhanced Mixing on a Centrifugal Platform

Robert Burger <sup>1,†</sup>, David J Kinahan <sup>2,3,†</sup> , Hélène Cayron <sup>4</sup>, Nuno Reis <sup>5</sup>, João Fonseca <sup>5</sup> and Jens Ducreé <sup>6,\*</sup> 

<sup>1</sup> BluSense Diagnostics, Fruebjergvej 3, DK-2100 København, Denmark; robert@blusense-diagnostics.com

<sup>2</sup> Advanced Processing Technology Research Center (APT), School of Mechanical Engineering, Dublin City University, 9 Dublin, Ireland; david.kinahan@dcu.ie

<sup>3</sup> Water Institute, Dublin City University, 9 Dublin, Ireland

<sup>4</sup> Biomedical Diagnostics Institute, Dublin City University, 9 Dublin, Ireland; helene.cayron@dcu.ie

<sup>5</sup> Biosurfit SA, Rua 25 de Abril n°66, 2050-317 Azambuja, Portugal; nunoreis@biosurfit.com (N.R.); joaofonseca@biosurfit.com (J.F.)

<sup>6</sup> Fraunhofer Project Center at Dublin City University (FPC@DCU), School of Physical Sciences, Dublin City University, 9 Dublin, Ireland

\* Correspondence: jens.ducree@dcu.ie; Tel.: +353-1-700-5299

† These authors contributed equally to this work.

Received: 2 December 2019; Accepted: 18 December 2019; Published: 22 December 2019



**Abstract:** We present a powerful and compact batch-mode mixing and dilution technique for centrifugal microfluidic platforms. Siphon structures are designed to discretize continuous flows into a sequence of droplets of volumes as low as 100 nL. Using a passive, self-regulating 4-step mechanism, discrete volumes of two fluids are alternately issued into a common intermediate chamber. At its base, a capillary valve acts as a fluidic shift register; a single droplet is held in place while two or more droplets merge and pass through the capillary stop. These merged droplets are advectively mixed as they pass through the capillary valve and into the receiving chamber. Mixing is demonstrated for various combinations of liquids such as aqueous solutions as well as saline solutions and human plasma. The mixing quality is assessed on a quantitative scale by using a colorimetric method based on the mixing of potassium thiocyanate and iron(III) chloride, and in the case of human plasma using a spectroscopic method. For instance, volumes of 5  $\mu$ L have been mixed in less than 20 s. Single-step dilutions up to 1:5 of plasma in a standard phosphate buffer solution are also demonstrated. This work describes the preliminary development of the mixing method which has since been integrated into a commercially available microfluidic cartridge.

**Keywords:** Lab-on-a-Chip; centrifugal microfluidics; Lab-on-a-Disc; mixing; siphon valves

## 1. Introduction

Microfluidics emerged as a significant area of research in the 1980s and early 1990s [1–5] driven by its promise to automate and miniaturize common but labor intensive laboratory tasks. Initial work overwhelmingly focused on chip-based analytical separations, e.g., capillary electrophoresis (CE) or high-performance liquid chromatography (HPLC), and the miniaturization of individual fluidic components such as pumps and valves through micromachining. In the recent decade there have been increasing efforts to apply ‘lab-on-a-chip’ to automating existing laboratory processes and to enable point-of-care/point-of-use distributed testing [6] and to leverage microfluidic physical effects to develop entirely new medical tools such as liquid biopsy [7] and exosome-based diagnostics [8].

Lab-on-a-chip platforms can be categorized on the basis of their underlying liquid handling principles such as electroosmosis, pressure, peristaltics, ultrasonics, and electrowetting. Centrifugal

microfluidic systems constitute a subset which uses the rotation of the chip, which is typically of a similar geometry as a Compact Disc™ or DVD™, to enable most pumping and valving operations. These systems can be further sub-divided into 'Bioanalytical Screening CDs' and 'Lab-on-a-Disc (LoaD)'. Bioanalytical screening CDs focus on adapting optical disc drive (ODD) technology (e.g., Compact Disc, DVD) for biological detection [9]. This technology takes advantage of the high-density data storage capability as well as the favorable pricing for its main constituents, i.e., the optical pickup unit, the spindle drive, and the optical disc substrates [10–14].

The LoaD [15–20] is typically used to automate the standard laboratory steps conducted in a biology lab to enable a fully automated sample-to-answer system. The LoaD is particularly applicable for deployment in the field (point-of-use) or at the hospital bed-side (point-of-care) as the chips can be loaded at atmospheric pressure (via pipette or syringe) without issues regarding sealing or priming. The use of centrifugation for pumping also reduces the cost and complexity of support instrumentation as just low-cost spindle motors are required rather than specialized micropumps. Similarly, inherent centrifugation of samples [21–23] applied to sample preparation is a particular strength.

The technological precursor of these systems are the centrifugal analyzers which became popular in the 1970s and 1980s [24] for automating a very limited number of simple assay steps, on rather macroscopic sample volumes, and readout on a rotor-based instrument. Currently the main areas of application are immunoassays [25–28], nucleic acid testing [29–36], and cell sorting/identification [37–43]. These lab-on-a-disc systems make specific use of the interplay of the frequency controlled centrifugal force and capillary action in a surface-functionalized network of micro-channels and cavities. Key liquid handling operations such as valving [44–48], metering [49,50], mixing [51,52], pumping [53–55], and switching/routing of flow [56,57] have been demonstrated.

A major challenge for microfluidic systems is rapid mixing. In general, one can categorize micromixers according to different characteristics [58,59], e.g., batch and continuous flow mode, laminar and turbulent, planar and 3-dimensional geometry, low- or high-aspect-ratio structures, manufacturing technologies or active/passive mixers. Active mixers utilize external stimuli such as ultrasonic waves [60], electrowetting [61] or periodically changing flow rates [62]. While it is hard to make a general statement, active mixers tend to significantly accelerate mixing; however, they are typically more complicated to fabricate and integrate, and more complex to control.

Passive mixers use the hydrodynamic energy, e.g., provided by a pressure difference created by a pump, gravity or centrifugal force, to restructure the liquid flows in such ways that fast mixing is promoted. Examples for passive mixing principles are bas-relief structures incorporated in the channel walls to induce advection in a liquid flow [63] and multi-lamination of flow [64], e.g., through split-and-recombine strategies [65,66].

Mixing principles using the specific effects on centrifugal lab-on-a-disc platforms [67] include Coriolis-force induced split-and-recombine [68], advection [69], reciprocating flow induced by centrifugo-pneumatic pumping [52,70], mixing enhanced by the Euler force through periodically changing angular acceleration [71,72] and/or magnetic beads [51], mixing by use of chemically generated bubbles [73], and mixing enhanced by deformation of soft chamber walls [74,75]. Mixing can also be enhanced through external pumping such as provision of external air sources [76,77]. These technologies are critically appraised in Table 1.

In this paper we present and characterize a passive, batch-mode, siphon-based mixer on a centrifugal microfluidic lab-on-a-disc platform. The system first uses a novel, siphon-based structure to discretize reagent into droplets of defined volumes which are transferred into an intermediate chamber. A capillary valve at the base of this intermediate chamber acts as a fluidic shift register; a single droplet is held in place while two or more droplets merge and pass through the capillary stop. The merged droplets are advectively mixed as they pass through the capillary valve and into the receiving chamber. The mixer enhances mixing while requiring a comparatively small footprint, thus saving precious real estate on the disc substrate.

Along with fluidic functionality, it is critically important that Lab-on-a-Disc cartridges be amenable to mass manufacturing techniques such as injection molding [78]. This work describes the initial development of this mixing structure and the primary manufacturing method, hot embossing, was selected to ensure the designs could easily be translated for manufacture by injection molding. The mixing structure presented here has since been integrated into an injection molded microfluidic cartridge by Biosurfit SA [79] and is now sold commercially.

**Table 1.** Comparison of Mixing Mechanisms in Centrifugal Microfluidics.

Description	Advantages	Disadvantages	References
<b>Microchannels-based</b> Liquid is split-and-recombined or flows through channels of specific orientations to induce secondary flows to increase the boundary area across which diffusion occurs.	Largely passive; Improves mixing speed.	Can occupy significant disc space; functions best with continuous flow	[68,69]
<b>Euler Force (Shake-mode)</b> Use of Euler force (disc acceleration and deceleration) to induce mixing. Can be combined with pneumatic chambers in enhance liquid displacement/reciprocating flows.	Fast mixing mechanism. Does not require additional support instrumentation.	Can occupy significant disc space. Requires a specific disc spin profile (i.e., acceleration and deceleration).	[52,70–72]
<b>Mixing by bubbles.</b> Provision of sources of pressurized air by on-rotor pneumatic pumps, via pneumatic slip-rings or through directing off-disc compressed air to generate air bubbles to enhance mixing. Use of chemical reactions to create bubbles.	Mechanism largely independent of disc spin-rate. Very rapid mixing mechanism.	Supporting instrumentation is complex and moves away from principal of Lab-on-a-Disc based solely on low-cost spindle motor. Can require specific chemical reagents stored on disc.	[73,76,77]
<b>Wall deformation</b> Mixing is enhanced by deforming chamber walls to induce liquid movement.	Mechanism largely independent of disc spin-rate.	Can require additional equipment such as magnet embedded in disc wall. Suitable only for discs made from soft material such as PDMS.	[74,75]

## 2. Materials and Methods

### 2.1. Method of Operation

We pursue a novel, 4-step concept to create alternating lamellae for rapid mixing on a centrifugal microfluidic platform:

1. Discretization of continuous flow by siphon mechanism into droplets
2. Merging of droplets in the intermediate chamber as enabled by the microfluidic shift register
3. Mixing of reagents upstream and during transfer through the capillary valve
4. Mixing enhanced by droplet impact on liquid interface in the outer chamber

The droplet formation in the first step is implemented by siphon-induced flow discretization (Figure 1). Liquid is centrifugally driven into a retention chamber at a flow rate,  $Q_i$ , scaling with the square of the rotational frequency (Figure 1a). The outlet of this first chamber is connected to a siphon. Given that the frequency dependent centrifugal field suppresses capillary priming of the siphon channel, liquid will continuously fill the chamber (Figure 1b) until the liquid level rises beyond the crest point of the siphon (i.e., the most radially inward point on the siphon). By definition of this design, as the liquid reaches the crest-point the siphon-based valve primes and releases liquid stored in the retention chamber at a mean outgoing flow rate  $Q_o$  (Figure 1c). If the respective flow resistances of the inlet and outlet sections of the siphon are properly chosen, i.e.,  $Q_o$  exceeds  $Q_i$ , the retention

chamber empties and the intrusion of gas disrupts the continuous liquid column which results in a droplet being issued into the mixing chamber (Figure 1d). At this point, the flow-discretization cycle reinitiates and the siphon acts again as a closed valve until the crest point is reached.

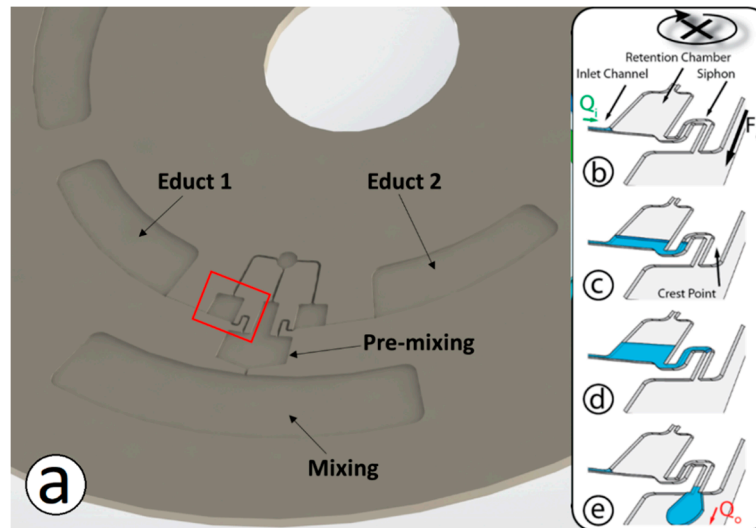


**Figure 1.** Working principle of the flow discretization structure. Subfigure (a) shows 1/3rd of a typical disc. Discs are manufactured to contain three identical mixing structures. The primary chambers are also labelled. Subfigures (b–e) illustrate the flow break-up principle. Under the impact of the centrifugal field, liquid flows through an inlet channel at a flow rate  $Q_i$  into the retention chamber (b) where it accumulates (c). Once the liquid level has passed the crest point of the siphon, the valve opens and liquid exits at a flow rate  $Q_o$  (d). When the chamber is empty, the liquid column breaks and the cycle resumes (e).

The size of the individual droplets is determined by the aggregate volume of the retention chamber  $V_c$  and the connected siphon up to the crest point  $V_s$  (Figure 2). These volumes can easily be adjusted in the layout to deliver the desired droplet volumes. The smallest droplet volumes can be obtained by eliminating the retention chamber and connecting the siphon directly to the inlet channel. The droplet volumes studied in this paper range from 100 nL to 890 nL.

In the second step, droplets emerging from the two inlets dispensed into a common intermediate/pre-mixing chamber (Figure 1). Single droplets (from either inlet) are retained in the intermediate chamber by capillary force as the centrifugal force is not sufficient to pump them through the outlet into the main mixing chamber. However, two or more droplets will merge at this point, overcome the capillary force, and transfer into the main mixing chamber. The intermediate chamber therefore acts analogous to a microfluidic shift register.

It should be noted that empirical observation shows that the siphons prime and dispense droplets in a phase-locked manner with alternate dispensing (i.e., a 180° phase shift) and this behavior is observed in all tests. Even though this was not an original design goal, this effect fortuitously enhances mixing efficiency. The authors surmise that the introduction of a droplet into the pre-mixing chamber creates a slight back pressure on the other siphon to induce the alternating dispensing.

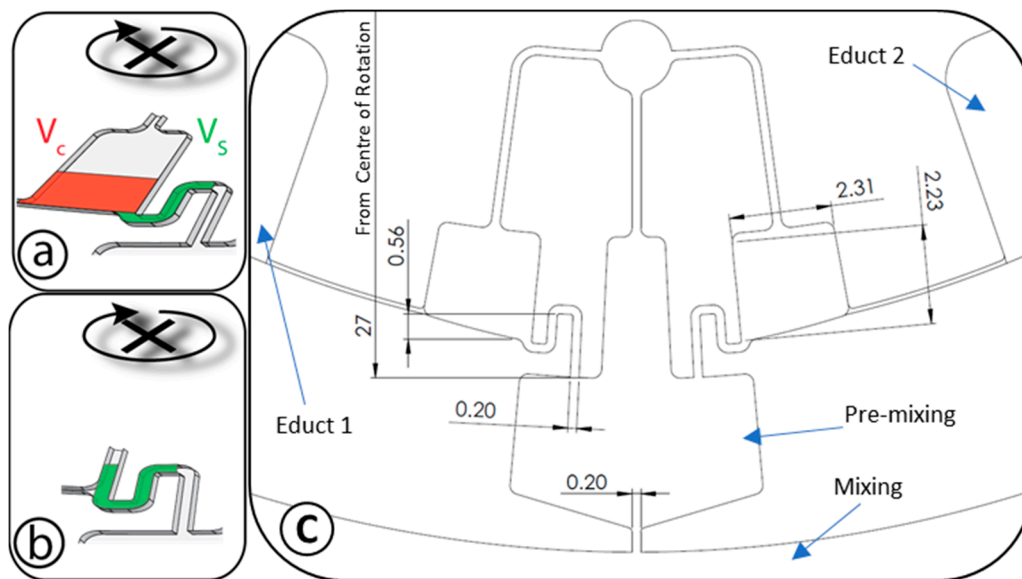


**Figure 2.** Relation of the droplet volume with the geometry of the retention chamber. (a) Chamber with attached outlet siphon. (b) The chamber is eliminated to minimize the droplet volume. (c) Shows the typical dimensions of a representative structure (in mm). Design files used in this paper (dxf) are provided in ESI.

The key impact parameters of the centrifugal mixer are the statically defined volume of the siphon and the connected chamber, the flow resistances of the inlet and outlet sections of the retention chamber and the nozzle channel, the lateral cross section of the common mixing chamber as well as the dynamically adjustable rotational frequency  $\omega$ .

Assuming laminar conditions in the common mixing chamber, Fick's law implies that the mixing time

$$t_{\text{mix}} \sim l^2/D \quad (1)$$

scales with the square of the layer thickness  $l$  and the inverse of the diffusion coefficient  $D$ . Assuming ideal, planar spreading upon impact, the layer thickness,  $l$ , depends on the droplet volume and the lateral extension (i.e., the width and the depth) of the mixing chamber. The mixing performance is not directly linked to the volume flow rate if the time period between two subsequent droplets is sufficiently large to allow lateral spreading.

To avoid the formation of a large single layer with long diffusion lengths at the end of the lamination process, it is important that both educt reservoirs are depleted at roughly the same instant in time. The time for the delivery of the entire liquid volume

$$t = V_{\text{educt}}/Q_i \quad (2)$$

corresponds to the quotient of the initial volume  $V_{\text{educt}}$  and the discharge flow rate  $Q_i$ , which, in turn, is given by the equivalent hydrostatic pressure difference  $\Delta P_\omega$  divided by the flow resistance of the inlet section  $R_{\text{hd}}$ .

$$Q_i = \Delta P_\omega / R_{\text{hd}} \quad (3)$$

The hydrostatic pressure difference  $\Delta P_\omega$  is given by

$$\Delta P_\omega = \rho \bar{r} \Delta r \omega^2 \quad (4)$$

with the density  $\rho$ , the mean radial position  $\bar{r}$  and radial length  $\Delta r$  of the liquid volume in the educt chamber.

Finally, the hydraulic resistance of a square channel can be approximated by:

$$R_{hd} = \frac{8 (1 + A_r)^2 \eta_l l}{A_r A^2} \quad (5)$$

with  $\eta_l$  being the viscosity of the liquid,  $A_r$  the aspect ratio of the channel and  $A$  its cross-sectional area.

## 2.2. Materials and Fabrication

Discs have been manufactured using two different methods, direct fabrication in dry film resist (DFR) (Figure 3) and hot embossing (Figure 4).

The masters for hot embossing have been created using SU-8 on a mask aligner (MA 56, Karl Süss, Garching, Germany). Different grades of SU8 were used in order to achieve different thicknesses of layers. SU8 3005 was used to make a base adhesion layer because, during initial testing, it was identified that small structures delaminated from the silicon wafer during hot-embossing. This SU8 base layer therefore increased the lifetime of the hot-embossing tool by providing an adhesive layer. SU8 3025 was used for the syphons and channels to achieve a depth of 30  $\mu\text{m}$  deep. SU8 3050 was used to create the reservoirs. In this case two layers are used to achieve the necessary depth for the reservoirs.

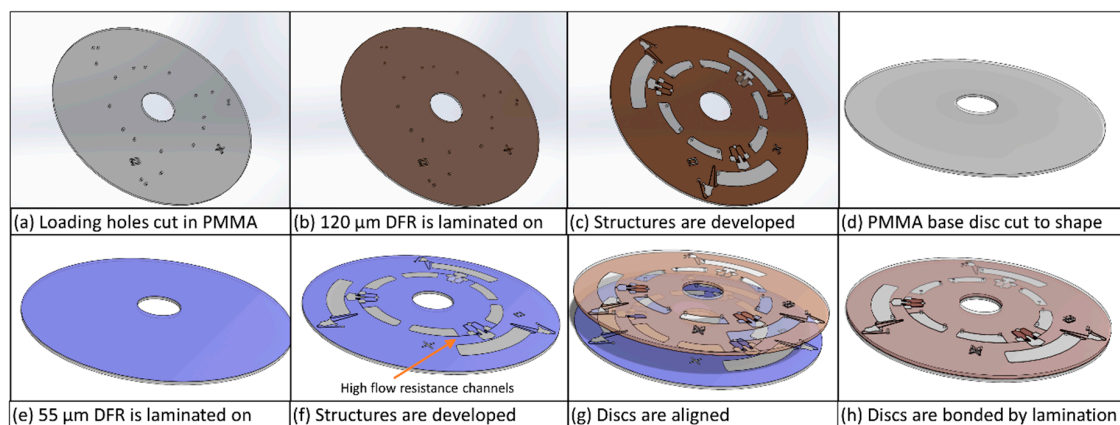


**Figure 3.** Schematic of the process for direct fabrication in dry film resist (DFR). 120  $\mu\text{m}$  Dry Film Resist (DFR) (Ordyl P50120, Elga Europe, Milan, Italy) is represented by the red material and 55  $\mu\text{m}$  DFR (SY 350, Elga Europe, Italy) by the blue material. The high flow resistance channels between the educt chambers and the discretization chambers are only present in the 55  $\mu\text{m}$  DFR. DFR is applied, and the final assembly bonded, by hot-roll lamination. Structures are cured and developed according to the manufacturers' protocols.

To this end first the first layer of SU-8 3005 (Microchem, Westborough, MA, USA) was spin coated on a silicon wafer at 2500 RPM, baked for 10 min at 95  $^{\circ}\text{C}$ , and subsequently been flood exposed at 200  $\text{mJ cm}^{-2}$  per manufacturers recommendation. This layer serves to improve the adhesion of the subsequent layers and hence increase the life time of the master. A second layer of SU-8 3025 was then spin coated with a thickness of 30  $\mu\text{m}$ , baked for 15 min at 95  $^{\circ}\text{C}$  and structured with an exposure energy of 240  $\text{mJ cm}^{-2}$ . Following a post exposure bake of 3 min at 95  $^{\circ}\text{C}$  a third layer of SU-8 3050 with a thickness of 170  $\mu\text{m}$  was spin-coated in two steps. After each step, the resist was baked at 95  $^{\circ}\text{C}$  for 20 min. The resist was then structured with an exposure intensity of 300  $\text{mJ cm}^{-2}$ . Subsequently, post exposure bake was performed at 95  $^{\circ}\text{C}$  for 6 min, followed by removal of unexposed resist in standard developer solution. The resist was then hard baked at 150  $^{\circ}\text{C}$  for 90 min. To facilitate demolding of the master after hot embossing the surface of the master was coated with a layer of Octadecyltrichlorosilane (OTS) (Sigma-Aldrich, Wicklow, Ireland). The coating has been created by immersing the wafer in a solution of 400  $\mu\text{M}$  of OTS in heptane (Sigma-Aldrich, Wicklow, Ireland)



for 120 min. Subsequently the master was sonicated in heptane for 5 min, followed by rinsing with methanol and finally baked on a hot plate at 100 °C for 20 min. This resulted in a hydrophobic surface coating with a water contact angle of approximately 108° and significantly facilitated demolding as compared to untreated masters.

Discs were embossed in 2-mm thick PMMA sheets (Radionics, Dublin, Ireland) using a HEX-02 hot embosser (Jenoptik, Jena, Germany) at a pressure of 2.85 MPa and an embossing temperature of 123 °C. The best pattern transfer was achieved with an embossing time of 310 s. The total cycle time was 15 min, only. Figure 4 shows a comparison of the master profile and the replicated PMMA disc.

After embossing, fluidic inlets were drilled ( $\varnothing$  1.3 mm) on a tower-drill and the discs were sealed by bonding to a PMMA disc using pressure sensitive adhesive (Adhesive Research, Limerick, Ireland).

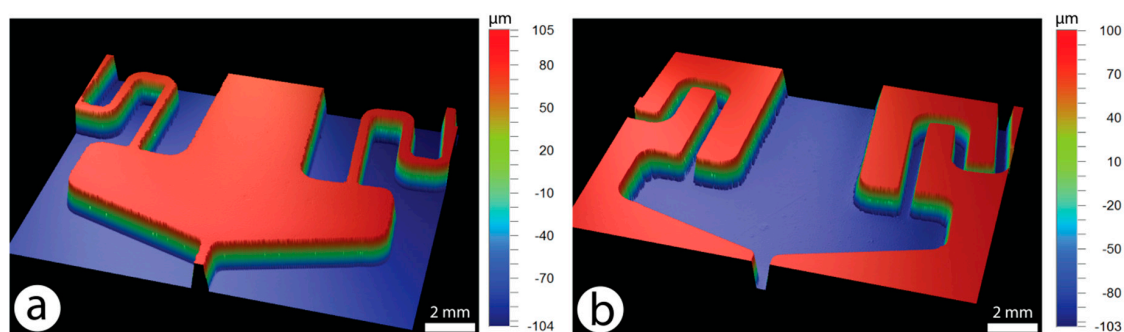


**Figure 4.** Profiles, acquired using a profilometer (Dektak 150), of (a) SU-8 master used for embossing and (b) profile of embossed PMMA mixing structure.

Discs for the asymmetric mixing of PBS buffer and plasma were manufactured using dry film resist (DFR) (Figure 3). A CO<sub>2</sub> laser (Epilog, Golden, CO, USA) was used to cut the PMMA substrates to disc shape and create fluidic I/O ports. Subsequently a layer of 120-µm thick DFR (Ordyl P50120, Elga Europe, Italy) was laminated onto the PMMA disc and structured with the reservoirs and mixing structure by exposure to UV light. The connecting channels between educt reservoirs and discretization chambers were created in 55-µm thick DFR (SY 350, Elga Europe, Italy) laminated on a 600-µm thick polycarbonate disc. After removing unexposed areas of DFR, both parts were aligned and bonded by lamination at 80 °C.

### 2.3. Measurement and Testing

The spin-stand [80] used to perform the fluidic experiments consists of a computer-controlled motor for spinning the discs (Faulhaber Minimotor SA, Croglio, Switzerland), a stroboscopic illumination (Drello, Mönchengladbach, Germany) and a highly sensitive color camera (Pixelfly qe, PCO, Kelheim, Germany) attached to a motorized 12× zoom lens (Navitar, Rochester, NY, USA).

In all cases liquid was loaded into the reservoirs by pipetting. The efficacy of mixing of potassium thiocyanate and iron(III) chloride was evaluated using a colorimetric method. Subsequent to mixing, an image of the resulting mixture was acquired using the camera of the test point setup. Using an image processing software (ImageJ, NIH, Washington, DC, USA), the area containing the mixture was selected and the standard deviation of the histogram was calculated. Since the supply reservoirs did not always empty simultaneously, the area where droplets were issued into the mixing reservoir was excluded from this analysis when it only contained one type of educt. To compensate systematic errors due to the measurement setup, the standard deviation of a reference mixture was recorded and later used to normalize the standard deviations measured during the experiments. The reference solution was prepared by mixing equal volumes of potassium thiocyanate and iron(III) chloride solution using a vortex mixer. Then the same amount of reference solution used in the mixing experiments was pipetted into an identical disk device and an image was acquired.

In experiments where plasma and PBS were mixed, a modified version of the structure was used (Figure 5). The mixing chamber is connected to a siphon which in turn leads to a sample collection reservoir. After performing the mixing, the disc is stopped to prime the siphon. The disc is then spun again, and a part of the mixture is transferred to the sample collection reservoir while monitoring the liquid level in the collection reservoir using the camera. The disc is stopped and a 1.5- $\mu\text{L}$  sample is collected from the reservoir and stored for further analysis. It took approximately 6–8 s to generate 1.5  $\mu\text{L}$  of sample for testing. The sampling step is repeated until all mixed liquid is collected. The mixing quality of each 1.5- $\mu\text{L}$  sample is then assessed using a spectrophotometer (Nanodrop 1000, Thermo Scientific, Waltham, MA, USA). The concentration of plasma proteins in each of these aliquots was determined by measuring the absorbance at 280 nm. A homogenous mixture would display the same concentration of proteins in all aliquots. Typically, 7–9 aliquots were collected per mixing trial.

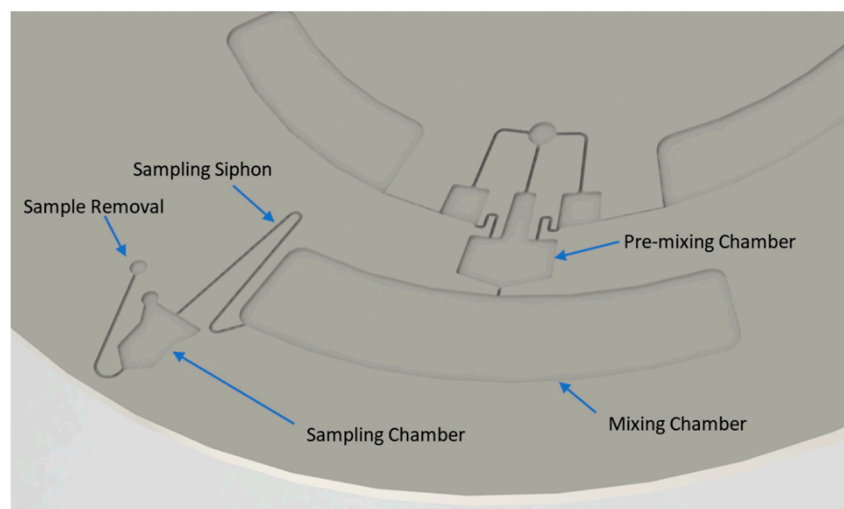


**Figure 5.** Representation of modified structure used to aliquot samples of plasma/PBS mixture. After mixing is complete disc is stopped to allow Sampling siphon to prime. Disc is then rotated to transfer 1.5  $\mu\text{L}$  into sampling chamber (i.e., lower part of sampling chamber is filled). This sample is then removed from sampling chamber and process is repeated until mixing chamber is emptied.

### 3. Results

All mixing experiments presented in this work have been carried out at rotation frequencies between 40 Hz and 50 Hz. The quality was evaluated immediately after mixing. At first, mixing of symmetric droplet volumes has been examined using four different structures which allow dispensing of different liquid volumes  $V_c + V_s$  (Figure 2): 170 nL, 240 nL, 420 nL, and 890 nL. All experiments have been performed with 5  $\mu\text{L}$  of each educt and mixing has been performed in less than 20 s.

A frame sequence obtained while dispensing discrete 170 nL volumes (Figure 6). The photos visualize the alternating dispensing of educt droplets from the flow discretization siphons, pre-mixing and dispensing of the droplets into the mixing chamber.



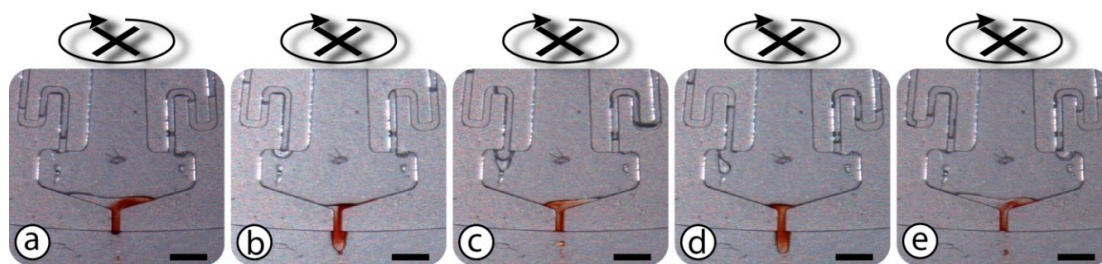


**Figure 6.** The image sequences show the droplet dispensing and pre-mixing process. Educts enter the siphon channels (a). The liquids are alternatingly issued into the common chamber with the nozzle outlet where the educts are pre-mixed before being dispensed through the nozzle into the mixing chamber (b–e). Images shown are acquired in time-steps of approximately 0.6 s.

The results of the mixing experiments with potassium thiocyanate and iron(III) chloride (Figure 7) confirm that, as expected, a reduced droplet size leads to faster mixing due to shorter diffusion distances.

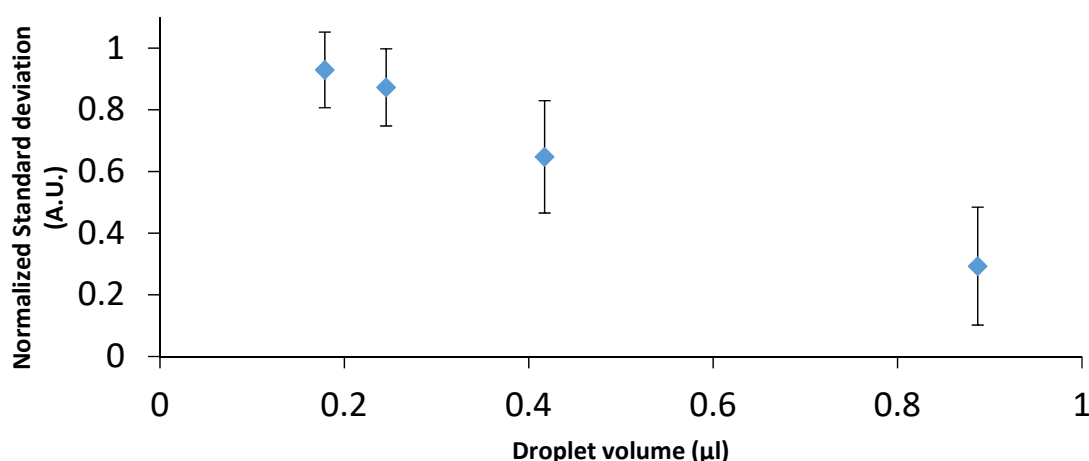


**Figure 7.** Normalized standard deviation of mixed aqueous solutions as a function of the droplet size provided by the two disc-based siphons. A value of unity corresponds to perfect mixing. The measured standard deviations were calibrated against the standard deviation of a sample processed by a conventional vortex mixer.

As expected, decreasing the droplet volumes improves homogeneity of the mixing. Furthermore, the mixing quality obtained with the smallest droplet volumes is close to the reference mixture.

Based on the outcomes of these experiments, mixing structures for the dilution of plasma have been designed. Since the smallest droplets delivered the best mixing quality, a discretization volume of 100 nL was chosen for the plasma dilution structure. We examined dilutions of plasma in PBS in ratios of 1:2.6 and 1:5, whereas the hydraulic resistance of the connecting channels was adjusted such that both liquid reservoirs emptied concurrently. Hydraulic resistances have been calculated based on the theory detailed above and channel parameters have been optimized experimentally. In Figure 8, the histograms show the distribution of the protein concentration in the aliquots collected over several experiments. Ideally, the concentration of all aliquots would be identical. These results demonstrate that the here proposed approach is well suitable for diluting human blood plasma in PBS.

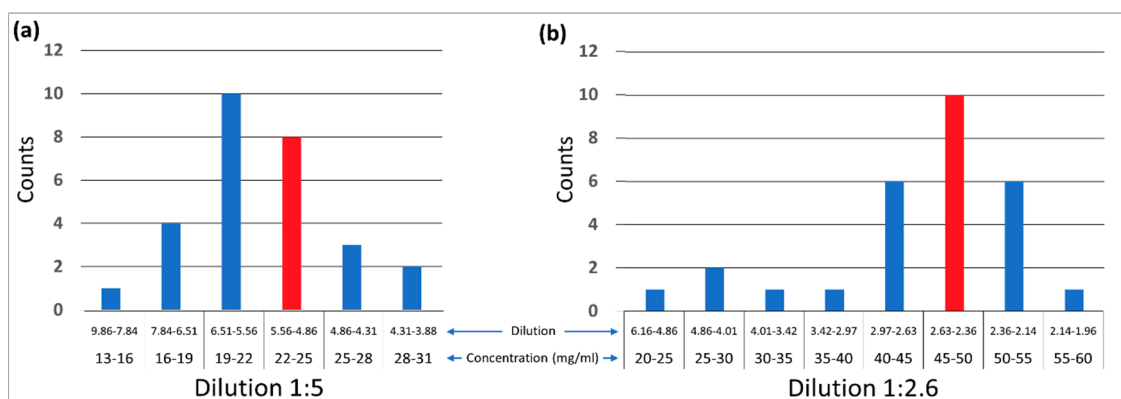


**Figure 8.** Results of mixing experiments with blood plasma and PBS buffer for two different mixing ratios. Histogram (a) shows the concentration distribution for a dilution of 1:5, while histogram (b) displays the distribution for a mixing ratio of 1:2.6. The red bars indicate the populations with the target dilution.

#### 4. Discussion and Conclusions

This work presents the preliminary studies used to develop a microfluidic mixing structure which has since been developed and sold commercially. The structure presented here exploits siphon-induced flow discretization to perform batch-mode mixing and dilution of liquids in a compact, small-footprint structure on a centrifugal microfluidic “Lab-on-a-Disc” platform. The specific architecture presented here is suitable for mixing liquids at ratios between unity and 1:5. It should be noted that, in the scope of this study, we only surmise the phase-locking of droplet creation, which is key to the system’s performance, is caused by pneumatic back-pressure in our system. Confirmation this mechanism exists, and full understanding of it through numerical simulation and further experimentation, will be key to identifying design improvements which can increase the speed and efficiency of our mixing structure.

Of critical importance to the commercialization of this technology is that it does not require surface modification and it functions at a constant spin rate. Independence from surface modification simplifies manufacturing and reduces cost. It also increases the number of materials from which the cartridges can be manufactured. Operating the mixing at a constant spin-rate makes it easier to implement functions in parallel such as filling a detection chamber with a calibration liquid or the reconstitution of dry reagents.

Furthermore, our structure has proven to be suitable for mixing liquids with considerably different hydrodynamic properties, such as human blood plasma and standard buffer solutions. In fact, in its commercial realization by Biosurfit SA, this structure has been adapted to generate plasma dilutions of 1:20 and 1:40. The structures presented in this paper were successfully prototyped using hot embossing to ensure the design was amenable to large scale production techniques such as injection molding. Since then, Biosurfit SA have produced and sold many thousands of injection molded Lab-on-a-Disc cartridges which use these structures for mixing.

**Author Contributions:** Conceptualization, R.B., H.C., N.R., J.F., and J.D.; methodology, R.B. and J.D.; formal analysis, R.B. and D.J.K.; investigation, R.B. and H.C.; resources, N.R., J.F., and J.D.; writing—original draft preparation, D.J.K. and R.B.; writing—review and editing, J.D.; supervision, J.D.; funding acquisition, J.D. All authors have read and agreed to the published version of the manuscript.

**Funding:** This work was funded by Science Foundation Ireland (SFI) under grant no 10/CE/B1821, and by SFI and Fraunhofer Gesellschaft under Grant No 16/SPP/3321.

**Conflicts of Interest:** The authors declare no conflict of interest.

## References

1. Dittrich, P.S.; Tachikawa, K.; Manz, A. Micro total analysis systems. Latest advancements and trends. *Anal. Chem.* **2006**, *78*, 3887–3908. [[CrossRef](#)] [[PubMed](#)]
2. Craighead, H. Future lab-on-a-chip technologies for interrogating individual molecules. In *Nanoscience and Technology: A Collection of Reviews from Nature Journals*; World Scientific: Singapore, 2010; pp. 330–336.
3. Demello, A.J. Control and detection of chemical reactions in microfluidic systems. *Nature* **2006**, *442*, 394–402. [[CrossRef](#)] [[PubMed](#)]
4. Whitesides, G.M. The origins and the future of microfluidics. *Nature* **2006**, *442*, 368. [[CrossRef](#)] [[PubMed](#)]
5. Mark, D.; Haeberle, S.; Roth, G.; Von Stetten, F.; Zengerle, R. Microfluidic lab-on-a-chip platforms: Requirements, characteristics and applications. In *Microfluidics Based Microsystems*; Springer: Berlin/Heidelberg, Germany, 2010; pp. 305–376.
6. Darwish, N.T.; Sekaran, S.D.; Khor, S.M. Point-of-care tests: A review of advances in the emerging diagnostic tools for dengue virus infection. *Sens. Actuators B Chem.* **2018**, *255*, 3316–3331. [[CrossRef](#)]
7. Alix-Panabières, C.; Pantel, K. Circulating tumor cells: Liquid biopsy of cancer. *Clin. Chem.* **2013**, *59*, 110–118. [[CrossRef](#)] [[PubMed](#)]
8. Avella-Oliver, M.; Puchades, R.; Wachsmann-Hogiu, S.; Maquieira, A. Label-free SERS analysis of proteins and exosomes with large-scale substrates from recordable compact disks. *Sens. Actuators B Chem.* **2017**, *252*, 657–662. [[CrossRef](#)]
9. Burger, R.; Amato, L.; Boisen, A. Detection methods for centrifugal microfluidic platforms. *Biosens. Bioelectron.* **2016**, *76*, 54–67. [[CrossRef](#)]
10. Barathur, R.; Bookout, J.; Sreevatsan, S.; Gordon, J.; Werner, M.; Thor, G.; Worthington, M. New disc-based technologies for diagnostic and research applications. *Psychiatr. Genet.* **2002**, *12*, 193–206. [[CrossRef](#)]
11. Lange, S.A.; Roth, G.; Wittemann, S.; Lacoste, T.; Vetter, A.; Grässle, J.; Kopta, S.; Kolleck, M.; Breiting, B.; Wick, M. Measuring biomolecular binding events with a compact disc player device. *Angew. Chem. Int. Ed.* **2006**, *45*, 270–273. [[CrossRef](#)]
12. Arai, T.; Gopinath, S.C.B.; Mizuno, H.; Kumar, P.K.R.; Rockstuhl, C.; Awazu, K.; Tominaga, J. Toward biological diagnosis system based on digital versatile disc technology. *Jpn. J. Appl. Phys.* **2007**, *46*, 4003. [[CrossRef](#)]
13. Morais, S.; Carrascosa, J.; Mira, D.; Puchades, R.; Maquieira, A. Microimmunoanalysis on standard compact discs to determine low abundant compounds. *Anal. Chem.* **2007**, *79*, 7628–7635. [[CrossRef](#)] [[PubMed](#)]
14. Wang, X.; Zhao, M.; Nolte, D.D. Combined fluorescent and interferometric detection of protein on a BioCD. *Appl. Opt.* **2008**, *47*, 2779–2789. [[CrossRef](#)] [[PubMed](#)]
15. Schembri, C.T.; Burd, T.L.; Kopf-Sill, A.R.; Shea, L.R.; Braynin, B. Centrifugation and capillarity integrated into a multiple analyte whole blood analyser. *J. Anal. Methods Chem.* **1995**, *17*, 99–104. [[CrossRef](#)] [[PubMed](#)]
16. Madou, M.; Zoval, J.; Jia, G.; Kido, H.; Kim, J.; Kim, N. Lab on a CD. *Annu. Rev. Biomed. Eng.* **2006**, *8*, 601–628. [[CrossRef](#)] [[PubMed](#)]
17. Ducrée, J.; Haeberle, S.; Lutz, S.; Pausch, S.; Von Stetten, F.; Zengerle, R. The centrifugal microfluidic Bio-Disk platform. *J. Micromech. Microeng.* **2007**, *17*, S103. [[CrossRef](#)]
18. Gorkin, R.; Park, J.; Siegrist, J.; Amasia, M.; Lee, B.S.; Park, J.-M.; Kim, J.; Kim, H.; Madou, M.; Cho, Y.-K. Centrifugal microfluidics for biomedical applications. *Lab Chip* **2010**, *10*, 1758–1773. [[CrossRef](#)]
19. Strohmeier, O.; Keller, M.; Schwemmer, F.; Zehnle, S.; Mark, D.; von Stetten, F.; Zengerle, R.; Paust, N. Centrifugal microfluidic platforms: Advanced unit operations and applications. *Chem. Soc. Rev.* **2015**, *44*, 6187–6229. [[CrossRef](#)]
20. Smith, S.; Mager, D.; Perebikovsky, A.; Shamloo, E.; Kinahan, D.; Mishra, R.; Torres Delgado, S.; Kido, H.; Saha, S.; Ducrée, J.; et al. CD-based microfluidics for primary care in extreme point-of-care settings. *Micromachines* **2016**, *7*, 22. [[CrossRef](#)]
21. Kinahan, D.J.; Kearney, S.M.; Glynn, M.T.; Ducrée, J. Spira mirabilis enhanced whole blood processing in a lab-on-a-disk. *Sens. Actuators A Phys.* **2014**, *215*, 71–76. [[CrossRef](#)]
22. Haeberle, S.; Brenner, T.; Zengerle, R.; Ducrée, J. Centrifugal extraction of plasma from whole blood on a rotating disk. *Lab Chip* **2006**, *6*, 776–781. [[CrossRef](#)]

23. Kinahan, D.J.; Kearney, S.M.; Kilcawley, N.A.; Early, P.L.; Glynn, M.T.; Ducrée, J. Density-gradient mediated band extraction of leukocytes from whole blood using centrifugo-pneumatic siphon valving on centrifugal microfluidic discs. *PLoS ONE* **2016**, *11*, e0155545. [[CrossRef](#)] [[PubMed](#)]
24. Burtis, C.A.; Mailen, J.C.; Johnson, W.F.; Scott, C.D.; Tiffany, T.O.; Anderson, N.G. Development of a miniature fast analyzer. *Clin. Chem.* **1972**, *18*, 753–761. [[PubMed](#)]
25. Lai, S.; Wang, S.; Luo, J.; Lee, L.J.; Yang, S.-T.; Madou, M.J. Design of a compact disk-like microfluidic platform for enzyme-linked immunosorbent assay. *Anal. Chem.* **2004**, *76*, 1832–1837. [[CrossRef](#)] [[PubMed](#)]
26. Honda, N.; Lindberg, U.; Andersson, P.; Hoffmann, S.; Takei, H. Simultaneous multiple immunoassays in a compact disc-shaped microfluidic device based on centrifugal force. *Clin. Chem.* **2005**, *51*, 1955–1961. [[CrossRef](#)] [[PubMed](#)]
27. Inganäs, M.; Dérand, H.; Eckersten, A.; Ekstrand, G.; Honerud, A.-K.; Jesson, G.; Thorsén, G.; Söderman, T.; Andersson, P. Integrated microfluidic compact disc device with potential use in both centralized and point-of-care laboratory settings. *Clin. Chem.* **2005**, *51*, 1985–1987. [[CrossRef](#)] [[PubMed](#)]
28. Delgado, S.M.T.; Kinahan, D.J.; Sandoval, F.S.; Julius, L.A.N.; Kilcawley, N.A.; Ducrée, J.; Mager, D. Fully automated chemiluminescence detection using an electrified-Lab-on-a-Disc (eLoaD) platform. *Lab Chip* **2016**, *16*, 4002–4011. [[CrossRef](#)]
29. Peng, X.Y.L.; Li, P.C.H.; Yu, H.-Z.; Ash, M.P.; Chou, W.L.J. Spiral microchannels on a CD for DNA hybridizations. *Sens. Actuators B Chem.* **2007**, *128*, 64–69. [[CrossRef](#)]
30. Jia, G.; Ma, K.-S.; Kim, J.; Zoval, J.V.; Peytavi, R.; Bergeron, M.G.; Madou, M.J. Dynamic automated DNA hybridization on a CD (compact disc) fluidic platform. *Sens. Actuators B Chem.* **2006**, *114*, 173–181. [[CrossRef](#)]
31. Cho, Y.-K.; Lee, J.-G.; Park, J.-M.; Lee, B.-S.; Lee, Y.; Ko, C. One-step pathogen specific DNA extraction from whole blood on a centrifugal microfluidic device. *Lab Chip* **2007**, *7*, 565–573. [[CrossRef](#)]
32. Li, C.; Dong, X.; Qin, J.; Lin, B. Rapid nanoliter DNA hybridization based on reciprocating flow on a compact disk microfluidic device. *Anal. Chim. Acta* **2009**, *640*, 93–99. [[CrossRef](#)]
33. Bañuls, M.-J.; García-Piñón, F.; Puchades, R.; Maquieira, Á. Chemical derivatization of compact disc polycarbonate surfaces for SNPs detection. *Bioconjug. Chem.* **2008**, *19*, 665–672. [[CrossRef](#)] [[PubMed](#)]
34. Siegrist, J.; Gorkin, R.; Bastien, M.; Stewart, G.; Peytavi, R.; Kido, H.; Bergeron, M.; Madou, M. Validation of a centrifugal microfluidic sample lysis and homogenization platform for nucleic acid extraction with clinical samples. *Lab Chip* **2010**, *10*, 363–371. [[CrossRef](#)] [[PubMed](#)]
35. Yuan, D.; Kong, J.; Li, X.; Fang, X.; Chen, Q. Colorimetric LAMP microfluidic chip for detecting three allergens: Peanut, sesame and soybean. *Sci. Rep.* **2018**, *8*, 8682. [[CrossRef](#)] [[PubMed](#)]
36. Hoehl, M.M.; Weißert, M.; Dannenberg, A.; Nesch, T.; Paust, N.; von Stetten, F.; Zengerle, R.; Slocum, A.H.; Steigert, J. Centrifugal LabTube platform for fully automated DNA purification and LAMP amplification based on an integrated, low-cost heating system. *Biomed. Microdevices* **2014**, *16*, 375–385. [[CrossRef](#)]
37. Burger, R.; Kirby, D.; Glynn, M.; Nwankire, C.; O'Sullivan, M.; Siegrist, J.; Kinahan, D.; Aguirre, G.; Kijanka, G.; Gorkin, R.A. Centrifugal microfluidics for cell analysis. *Curr. Opin. Chem. Biol.* **2012**, *16*, 409–414. [[CrossRef](#)]
38. Morijiri, T.; Sunahiro, S.; Senaha, M.; Yamada, M.; Seki, M. Sedimentation pinched-flow fractionation for size-and density-based particle sorting in microchannels. *Microfluid. Nanofluidics* **2011**, *11*, 105–110. [[CrossRef](#)]
39. Lee, S.-W.; Kang, J.Y.; Lee, I.-H.; Ryu, S.-S.; Kwak, S.-M.; Shin, K.-S.; Kim, C.; Jung, H.-I.; Kim, T.-S. Single-cell assay on CD-like lab chip using centrifugal massive single-cell trap. *Sens. Actuators A Phys.* **2008**, *143*, 64–69. [[CrossRef](#)]
40. Chen, C.-L.; Chen, K.-C.; Pan, Y.-C.; Lee, T.-P.; Hsiung, L.-C.; Lin, C.-M.; Chen, C.-Y.; Lin, C.-H.; Chiang, B.-L.; Wo, A.M. Separation and detection of rare cells in a microfluidic disk via negative selection. *Lab Chip* **2011**, *11*, 474–483. [[CrossRef](#)]
41. Burger, R.; Reith, P.; Kijanka, G.; Akujobi, V.; Abgrall, P.; Ducrée, J. Array-based capture, distribution, counting and multiplexed assaying of beads on a centrifugal microfluidic platform. *Lab Chip* **2012**, *12*, 1289–1295. [[CrossRef](#)]
42. Burger, R.; Kurzbuch, D.; Gorkin, R.; Kijanka, G.; Glynn, M.; McDonagh, C.; Ducrée, J. An integrated centrifugo-opto-microfluidic platform for arraying, analysis, identification and manipulation of individual cells. *Lab Chip* **2015**, *15*, 378–381. [[CrossRef](#)]

43. Glynn, M.; Kirby, D.; Chung, D.; Kinahan, D.J.; Kijanka, G.; Ducrée, J. Centrifugo-magnetophoretic purification of CD4+ cells from whole blood toward future HIV/AIDS point-of-care applications. *J. Lab. Autom.* **2014**, *19*, 285–296. [[CrossRef](#)] [[PubMed](#)]
44. Lu, C.; Xie, Y.; Yang, Y.; Cheng, M.M.-C.; Koh, C.-G.; Bai, Y.; Lee, L.J.; Juang, Y.-J. New valve and bonding designs for microfluidic biochips containing proteins. *Anal. Chem.* **2007**, *79*, 994–1001. [[CrossRef](#)] [[PubMed](#)]
45. Chen, J.M.; Huang, P.-C.; Lin, M.-G. Analysis and experiment of capillary valves for microfluidics on a rotating disk. *Microfluid. Nanofluidics* **2008**, *4*, 427–437. [[CrossRef](#)]
46. Park, J.-M.; Cho, Y.-K.; Lee, B.-S.; Lee, J.-G.; Ko, C. Multifunctional microvalves control by optical illumination on nanoheaters and its application in centrifugal microfluidic devices. *Lab Chip* **2007**, *7*, 557–564. [[CrossRef](#)] [[PubMed](#)]
47. Delgado, S.M.T.; Kinahan, D.J.; Julius, L.A.N.; Mallette, A.; Ardila, D.S.; Mishra, R.; Miyazaki, C.M.; Korvink, J.G.; Ducrée, J.; Mager, D. Wirelessly powered and remotely controlled valve-array for highly multiplexed analytical assay automation on a centrifugal microfluidic platform. *Biosens. Bioelectron.* **2018**, *109*, 214–223. [[CrossRef](#)]
48. Kinahan, D.J.; Early, P.L.; Vembadi, A.; MacNamara, E.; Kilcawley, N.A.; Glennon, T.; Diamond, D.; Brabazon, D.; Ducrée, J. Xurography actuated valving for centrifugal flow control. *Lab Chip* **2016**, *16*, 3454–3459. [[CrossRef](#)]
49. Steigert, J.; Brenner, T.; Grumann, M.; Riegger, L.; Lutz, S.; Zengerle, R.; Ducrée, J. Integrated siphon-based metering and sedimentation of whole blood on a hydrophilic lab-on-a-disk. *Biomed. Microdevices* **2007**, *9*, 675–679. [[CrossRef](#)]
50. Mark, D.; Metz, T.; Haeberle, S.; Lutz, S.; Ducrée, J.; Zengerle, R.; von Stetten, F. Centrifugo-pneumatic valve for metering of highly wetting liquids on centrifugal microfluidic platforms. *Lab Chip* **2009**, *9*, 3599–3603. [[CrossRef](#)]
51. Grumann, M.; Geipel, A.; Riegger, L.; Zengerle, R.; Ducrée, J. Batch-mode mixing on centrifugal microfluidic platforms. *Lab Chip* **2005**, *5*, 560–565. [[CrossRef](#)]
52. Noroozi, Z.; Kido, H.; Micic, M.; Pan, H.; Bartolome, C.; Princevac, M.; Zoval, J.; Madou, M. Reciprocating flow-based centrifugal microfluidics mixer. *Rev. Sci. Instrum.* **2009**, *80*, 75102. [[CrossRef](#)]
53. Zehnle, S.; Roth, G.; von Stetten, F.; Roland, Z.; Paust, N. Centrifugo-dynamic inward pumping of liquids on a centrifugal microfluidic platform. *Lab Chip* **2012**, *12*, 5142–5145. [[CrossRef](#)] [[PubMed](#)]
54. Gorkin, R., III; Clime, L.; Madou, M.; Kido, H. Pneumatic pumping in centrifugal microfluidic platforms. *Microfluid. Nanofluidics* **2010**, *9*, 541–549. [[CrossRef](#)]
55. Miyazaki, C.M.; Kinahan, D.J.; Mishra, R.; Mangwanya, F.; Kilcawley, N.; Ferreira, M.; Ducrée, J. Label-free, spatially multiplexed SPR detection of immunoassays on a highly integrated centrifugal Lab-on-a-Disc platform. *Biosens. Bioelectron.* **2018**, *119*, 86–93. [[CrossRef](#)] [[PubMed](#)]
56. Brenner, T.; Glatzel, T.; Zengerle, R.; Ducrée, J. Frequency-dependent transversal flow control in centrifugal microfluidics. *Lab Chip* **2005**, *5*, 146–150. [[CrossRef](#)]
57. Kinahan, D.J.; Kearney, S.M.; Dimov, N.; Glynn, T.; Ducrée, J. Event-triggered logical flow control for comprehensive process integration of multi-step assays on centrifugal microfluidic platforms. *Lab Chip* **2014**, *14*, 2249–2258. [[CrossRef](#)]
58. Nguyen, N.-T.; Wu, Z. Micromixers—A review. *J. Micromech. Microeng.* **2004**, *15*, R1. [[CrossRef](#)]
59. Hessel, V.; Löwe, H.; Schönfeld, F. Micromixers—A review on passive and active mixing principles. *Chem. Eng. Sci.* **2005**, *60*, 2479–2501. [[CrossRef](#)]
60. Yang, Z.; Goto, H.; Matsumoto, M.; Maeda, R. Active micromixer for microfluidic systems using lead-zirconate-titanate (PZT)-generated ultrasonic vibration. *Electrophor. Int. J.* **2000**, *21*, 116–119. [[CrossRef](#)]
61. Paik, P.; Pamula, V.K.; Fair, R.B. Rapid droplet mixers for digital microfluidic systems. *Lab Chip* **2003**, *3*, 253–259. [[CrossRef](#)]
62. Glasgow, I.; Aubry, N. Enhancement of microfluidic mixing using time pulsing. *Lab Chip* **2003**, *3*, 114–120. [[CrossRef](#)]
63. Stroock, A.D.; Dertinger, S.K.W.; Ajdari, A.; Mezić, I.; Stone, H.A.; Whitesides, G.M. Chaotic mixer for microchannels. *Science* **2002**, *295*, 647–651. [[CrossRef](#)] [[PubMed](#)]
64. Bessoth, F.G.; deMello, A.J.; Manz, A. Microstructure for efficient continuous flow mixing. *Anal. Commun.* **1999**, *36*, 213–215. [[CrossRef](#)]



65. Lee, S.W.; Kim, D.S.; Lee, S.S.; Kwon, T.H. A split and recombination micromixer fabricated in a PDMS three-dimensional structure. *J. Micromech. Microeng.* **2006**, *16*, 1067. [[CrossRef](#)]
66. Schönfeld, F.; Hessel, V.; Hofmann, C. An optimised split-and-recombine micro-mixer with uniform ‘chaotic’ mixing. *Lab Chip* **2004**, *4*, 65–69. [[CrossRef](#)] [[PubMed](#)]
67. Ren, Y.; Leung, W.W.-F. Numerical and experimental investigation on flow and mixing in batch-mode centrifugal microfluidics. *Int. J. Heat Mass Transf.* **2013**, *60*, 95–104. [[CrossRef](#)]
68. Ducrée, J.; Haeberle, S.; Brenner, T.; Glatzel, T.; Zengerle, R. Patterning of flow and mixing in rotating radial microchannels. *Microfluid. Nanofluidics* **2006**, *2*, 97–105. [[CrossRef](#)]
69. Ducree, J.; Brenner, T.; Haeberle, S.; Glatzel, T.; Zengerle, R. Multilamination of flows in planar networks of rotating microchannels. *Microfluid. Nanofluidics* **2006**, *2*, 78–84. [[CrossRef](#)]
70. Kinahan, D.J.; Kearney, S.M.; Faneuil, O.P.; Glynn, M.T.; Dimov, N.; Ducrée, J. Paper imbibition for timing of multi-step liquid handling protocols on event-triggered centrifugal microfluidic lab-on-a-disc platforms. *RSC Adv.* **2015**, *5*, 1818–1826. [[CrossRef](#)]
71. Haeberle, S.; Brenner, T.; Schlosser, H.; Zengerle, R.; Ducrée, J. Centrifugal micromixery. *Chem. Eng. Technol. Ind. Chem. Equip.-Process Eng.* **2005**, *28*, 613–616. [[CrossRef](#)]
72. Kuo, J.-N.; Li, Y.-S. Centrifuge-based micromixer with three-dimensional square-wave microchannel for blood plasma mixing. *Microsyst. Technol.* **2017**, *23*, 2343–2354. [[CrossRef](#)]
73. Burger, S.; Schulz, M.; von Stetten, F.; Zengerle, R.; Paust, N. Rigorous buoyancy driven bubble mixing for centrifugal microfluidics. *Lab Chip* **2016**, *16*, 261–268. [[CrossRef](#)] [[PubMed](#)]
74. Cai, Z.; Xiang, J.; Chen, H.; Wang, W. A rapid micromixer for centrifugal microfluidic platforms. *Micromachines* **2016**, *7*, 89. [[CrossRef](#)] [[PubMed](#)]
75. Burger, R.; Reith, P.; Akujobi, V.; Ducrée, J. Rotationally controlled magneto-hydrodynamic particle handling for bead-based microfluidic assays. *Microfluid. Nanofluidics* **2012**, *13*, 675–681. [[CrossRef](#)]
76. Kong, M.C.R.; Salin, E.D. Micromixing by pneumatic agitation on continually rotating centrifugal microfluidic platforms. *Microfluid. Nanofluidics* **2012**, *13*, 519–525. [[CrossRef](#)]
77. Clime, L.; Brassard, D.; Geissler, M.; Veres, T. Active pneumatic control of centrifugal microfluidic flows for lab-on-a-chip applications. *Lab Chip* **2015**, *15*, 2400–2411. [[CrossRef](#)]
78. Morelli, L.; Seriola, L.; Centorbi, F.A.; Jendresen, C.B.; Matteucci, M.; Ilchenko, O.; Demarchi, D.; Nielsen, A.T.; Zór, K.; Boisen, A. Injection molded lab-on-a-disc platform for screening of genetically modified E. coli using liquid–liquid extraction and surface enhanced Raman scattering. *Lab Chip* **2018**, *18*, 869–877. [[CrossRef](#)]
79. Da Fonseca, J.G.; Reis, N.A.E.; Burger, R. Analytical Rotors and Methods for Analysis of Biological Fluids. U.S. Patent 8,440,147, 14 May 2013.
80. Brennan, D.; Coughlan, H.; Clancy, E.; Dimov, N.; Barry, T.; Kinahan, D.; Ducrée, J.; Smith, T.J.; Galvin, P. Development of an on-disc isothermal in vitro amplification and detection of bacterial RNA. *Sens. Actuators B Chem.* **2017**, *239*, 235–242. [[CrossRef](#)]

